APPLIED AND ENVIRONMENTAL MICROBIOLOGY, Dec. 2001, p. 5410–5419 Vol. 67, No. 12
0099-2240/01/$04.00+0 DOI: 10.1128/AEM.67.12.5410–5419.2001

Motility of *Marichromatium gracile* in Response to Light, Oxygen, and Sulfide

ROLAND THAR* AND MICHAEL KÜHL

Marine Biological Laboratory, University of Copenhagen, DK-3000 Helsingør, Denmark

Received 9 July 2001/Accepted 7 September 2001

The motility of the purple sulfur bacterium *Marichromatium gracile* was investigated under different light regimes in a gradient capillary setup with opposing oxygen and sulfide gradients. The gradients were quantified with microsensors, while the behavior of swimming cells was studied by video microscopy in combination with a computerized cell tracking system. *M. gracile* exhibited photokinesis, photophobic responses, and phobic responses toward oxygen and sulfide. The observed migration patterns could be explained solely by the various phobic responses. In the dark, *M. gracile* formed an ~500-μm-thick band at the oxic-anoxic interface, with a sharp border toward the oxic zone always positioned at ~10 μM O_2. Flux calculations yielded a molar conversion ratio S_{tot}/O_2 of 2.03:1 (S_{tot} = $[H_2S]$ + $[HS^-]$ + $[S^{2-}]$) for the sulfide oxidation within the band, indicating that in darkness the bacteria oxidized sulfide incompletely to sulfur stored in intracellular sulfur globules. In the light, *M. gracile* spread into the anoxic zone while still avoiding regions with >10 μM O_2. The cells also preferred low sulfide concentrations if the oxygen was replaced by nitrogen. A light-dark transition experiment demonstrated a dynamic interaction between the chemical gradients and the cell's metabolism. In darkness and anoxia, *M. gracile* lost its motility after ca. 1 h. In contrast, at oxygen concentrations of >100 μM with no sulfide present the cells remained viable and motile for ca. 3 days both in light and darkness. Oxygen was respired also in the light, but respiration rates were lower than in the dark. Observed aggregation patterns are interpreted as effective protection strategies against high oxygen concentrations and might represent first stages of biofilm formation.

Purple sulfur bacteria perform anoxygenic photosynthesis utilizing reduced sulfur compounds as electron donors. Phototrophy is regarded as the ecologically most important mode of their metabolism (28). However, several species can grow chemotrophically under microaerobic conditions by respiring reduced sulfur compounds with molecular oxygen (21). Mass developments of purple sulfur bacteria are often observed in anaerobic water columns and in benthic habitats, where reduced sulfur compounds, as well as sufficient light intensity, are abundant. Such habitats can, for example, be found in the hypolimnion of stratified lakes (40) or in the upper millimeters of sulfidic sediment and microbial mats (28). Opposing sulfide and oxygen gradients characterize these ecological systems (19, 42).

The various light conditions during a diurnal cycle are accompanied by changes of the oxygen and sulfide distribution (19). Purple sulfur bacteria have adapted to such conditions by different strategies: the physiology of species such as *Thiocapsa roseopersicina* is adapted to withstand a wide range of environmental conditions (6, 33), whereas motile species follow their preferred environment by migration (13). The latter was reported for the gas-vacuolated species *Thiopedia rosea*, which is able to migrate in the water column of lakes by changing its buoyancy (23). Diurnal migration has also been reported for flagellated *Chromatium* spp. (the former genus *Chromatium* was recently reclassified into several new genera [17]). Sorokin (40) observed migration of these bacteria in Lake Belovod, whereas Jørgensen (19) described their motile behavior in sulfidic microbial mats dominated by *Oscillatoria* and *Beggiatoa* spp. During daytime *Chromatium* stayed below the oxic zone at a depth of ca. 2 mm. After sunset, the sulfidic zone expanded toward the mat surface, finally resulting in the release of sulfide into the overlying water. This process was accompanied by the migration of the *Chromatium* population into the sulfidic surface water. Soon after sunrise with the onset of oxygenic photosynthesis, the swarming bacteria retreated rapidly into the sediment.

The migration patterns found in nature should on principle be explainable by the chemotactic and phototactic behavior of the cells. Extensive studies exist about the characteristic photophobic step-down response of *Chromatium* spp. (termed by other authors "photophobotaxis"). If swimming cells experience diminishing light intensities, they stop and reverse their swimming direction, whereby *Chromatium* cells effectively accumulate at optimal irradiance (15, 16, 38). A combined effect of chemotaxis and photoresponses can be observed under the microscope. *Chromatium* cells accumulate around air bubbles in the absence of light but move away if illuminated (1) (an observation that has been erroneously cited to be already observed by Engelmann [9] in 1883). Beside the photophobic response, *Chromatium* exhibits also photokinesis (29), i.e., swimming velocities are correlated to the illumination intensity.

In recent years much progress has been made in understanding the molecular mechanisms behind the motile behavior of purple bacteria. The bacteria sense the rate of electron transfer in their electron transport chains (1). Phototactic and chemotactic signals are integrated, because photosynthesis and respiration share parts of their electron transport chains (37). Both processes compete for electrons, but photosynthesis is

* Corresponding author. Mailing address: Marine Biological Laboratory, University of Copenhagen, Strandpromenaden 5, DK-3000 Helsingør, Denmark. Phone: 45-49-21-33-44. Fax: 45-49-26-11-65. E-mail: roland.thar@gmx.net.

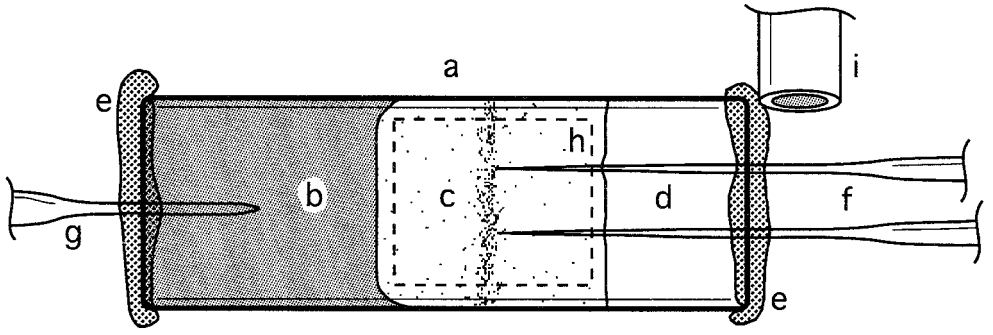

FIG. 1. Top view of gradient capillary setup with flat microslide capillary (8 by 0.8 by 40 mm^3) (a), sulfidic agar plug (b), motile bacteria in liquid medium (c), gas-filled space (d), Vaseline (e), microsensors (f), pH reference electrode (g), border of illuminated region (dashed line) (h), and the end of the tubing for flushing the capillary opening with defined gas mixtures (i).

preferred under electron donor-limiting conditions, and respiration rates decrease with increasing light intensities (5).

Our goal was to study and quantify the motility behavior of *Marichromatium gracile* in defined gradients and light regimes in order to explain how the behavior of single cells leads to the migration patterns observed in natural systems. We used a gradient capillary setup, which allowed the preparation of defined opposing sulfide and oxygen gradients inside a flat microslide capillary that could be illuminated with various light intensities. Chemical gradients and light fields inside the capillary were measured with microsensors, while tracks of individual bacteria in relation to light and chemical gradients could be analyzed via a computerized cell tracking system based on video microscopy. Similar gradient capillaries in combination with oxygen microsensor measurements and microscopy have been used previously for studies of motile colorless sulfur bacteria (11), ciliates (3), and sulfate-reducing bacteria (10).

MATERIALS AND METHODS

Sulfide nomenclature. The total sulfide concentration (S_{tot}) is calculated as follows:

$$S_{tot} = [H_2S] + [HS^-] + [S^{2-}] \quad (1)$$

The H_2S microsensor (see below) detects only $[H_2S]$ (18, 26). $[S^{2-}]$ can be neglected at pH values of <9. Thus, S_{tot} can be calculated from $[H_2S]$ and the pH value as follows (18):

$$S_{tot} = [H_2S] (1 + K_1/[H^+]) \quad (2)$$

where K_1 is the first dissociation constants of the sulfide equilibrium system, assuming a pK_1 of 7.05 (24).

Bacterial strain and culture condition. The purple sulfur bacterium *M. gracile* strain CE2205 (previously named *Chromatium gracile* and reclassified by Imhoff et al. [17]) was received from the culture collection of the Laboratory of Biological Oceanography, University Bordeaux I, Arcachon, France. The motile cells are ovoid to rod shaped, 1.0 to 1.4 μm by 2.2 to 4.5 μm, with polar flagellation. They grow phototrophically by utilizing sulfide, intracellular sulfur, or thiosulfate as the electron donor. Under microaerobic conditions, this species can also grow chemolithotrophically with oxygen as the electron acceptor (22).

Cultures were grown photoautotrophically under anaerobic condition with sulfide as electron donor at 25‰ salinity and 20°C in the medium described by Eichler and Pfennig (8). Illumination was provided by an incandescent lamp with a regime of 12 h of light and 12 h of dark. The applied scalar irradiance was 70 μmol of photons m^{-2} s^{-1} for visible light (400 to 700 nm) and 190 μmol of photons m^{-2} s^{-1} for near-infrared light (700 to 950 nm). When intracellular sulfur globules disappeared, cultures were refed with neutralized sulfide stock solution to a final S_{tot} of ca. 1 mM. All experiments were performed with cultures in their exponential growth phase and with all cells showing intracellular sulfur globules. The samples for the experiments were taken from the upper water column in the culture bottle in order to exclude nonmotile cells which aggregated at the bottom.

Gradient capillary setup. About one-half of a flat microslide capillary (internal dimensions 8 by 0.8 by 40 mm^3; VitroCom, Inc.) was filled with a sulfidic agar plug (Fig. 1). The 1% agar plug was prepared from filtered anoxic seawater (25‰ salinity) mixed with neutralized sulfide stock solution to a final concentration of 1 to 10 mM S_{tot}. The central part of the capillary was filled with liquid *M. gracile* culture by using a syringe connected to a hypodermic needle. Air bubbles were carefully avoided. The liquid culture extended over a distance of 7 to 10 mm between the agar plug and the meniscus. The inner walls of the remaining gas-filled part of the capillary were covered by a thin film of petroleum jelly (Vaseline; Chesebrough-Pond's, Inc.), ensuring that the meniscus of the liquid culture formed a straight line. Both openings of the capillary were closed with Vaseline in order to avoid evaporation. The composition of the gas in the gas-filled part could be controlled by flushing the surrounding of the opening with defined gas mixtures. The gas supply during the experiments was not limited by the Vaseline due to the high diffusivity of gases within Vaseline. The gradient capillary was mounted horizontally on the stage of a light microscope.

Capillaries with homogeneous sulfide or oxygen concentrations. Liquid cell culture was added to the central 10 mm of a flat microslide capillary (same dimensions as the gradient capillary). For anoxic sulfidic conditions both ends were closed with 1 mM S_{tot} agar plugs (as described above) and covered with Vaseline. For oxic conditions, the capillary was only closed with Vaseline, allowing for diffusion of oxygen into the liquid culture. The prepared capillaries were stored for ca. 1 h, whereafter the oxygen concentration in the capillary had increased to >100 μM and no free sulfide was detectable.

Illumination and irradiance measurements. The bright-field illumination of the microscope was used for illumination of the liquid culture within the gradient capillary. In order to avoid an inhomogeneous light field due to scattering or refraction at the borders, only the part indicated by the broken lines in Fig. 1 was illuminated by placing a quadratic field stop beneath the capillary. Scalar irradiance within the gradient capillary was measured with a microprobe consisting of a light-integrating sphere (70 μm in diameter) fixed to the light collecting end of a tapered optical fiber (27), which was connected to a light meter only sensitive to visible light (400 to 700 nm) with a flat spectral responsivity (25). The ratio between integral visible light (400 to 700 nm) and near-infrared light (700 to 950 nm) was 1:8.3, as measured in micromoles of photons per square meter per second with a fiber-optic spectrometer (Hamamatsu, Inc.). This ratio was kept constant throughout the experiments, and all irradiance values presented below are given as the scalar irradiance of the visible region.

Irradiances of >20 μmol of photons m^{-2} s^{-1} were not applied in the experiments in order to avoid an increase in temperature inside the gradient capillary. The irradiance was varied by placing neutral-density filters (Oriel, Inc.) into the illumination path. The filters were spectrally neutral to visible light and near-infrared light. Video microscopy for cell tracking during experiments in the dark (see below) was performed under weak red light (650 to 700 nm) by placing corresponding short-pass and long-pass interference filters (CVI, Inc.) into the illumination path. The red light apparently did not affect the swimming behavior of the bacteria, since shading did not cause a photophobic response.

Microsensor measurements. Dissolved oxygen measurements were done with Clark-type O_2 microsensors with a guard cathode (35) connected to a picoam-

meter (Unisense A/S). The microsensors had a tip diameter of 10 to 20 μm and <1 to 2% stirring sensitivity. A linear two-point calibration was performed from microsensor readings in seawater (25‰ salinity, 20°C) flushed with air and nitrogen, respectively.

Dissolved hydrogen sulfide was measured with amperometric H_2S microsensors (18, 26) connected to a picoammeter (Unisense A/S). The electrodes had a tip diameter of 10 to 20 μm and <1 to 2% stirring sensitivity. Calibration was performed in a closed glass vessel filled with anoxic phosphate buffer (50 mM, pH 7.0, 20°C). Sulfide standard stock solution (10 mM S_{tot}) was added to the buffer in several consecutive steps up to a final S_{tot} concentration of 0.5 mM (corresponding to $[H_2S] = 0.25$ mM). The obtained calibration points were fitted by linear regression. The linear equation obtained by the fitting procedure was used for converting the microsensor signal to H_2S concentrations. The exact molarity of the standard stock solution was determined by the titrimetric method described by Fonselius (12). S_{tot} profiles were calculated by equation 2 from measured $[H_2S]$ and pH (see below).

pH was measured with a potentiometric pH glass microsensor (36) connected to a high-impedance millivoltmeter (World Precision Instruments, Inc.). The pH-sensitive electrode tip had a length of ca. 100 μm and a diameter of ca. 20 μm. The reference electrode consisted of a chlorinated silver wire immersed into saturated KCl solution inside of a small capillary (tip diameter, ca. 0.5 mm). The pH microsensor was calibrated directly in the gradient capillary after the actual measurements were finished (see below) by replacing the liquid culture with standard buffer solutions of pH 7.0 and 11.0 for a linear two-point calibration.

Both the O_2 and the H_2S microsensor were mounted horizontally on a computer-controlled motorized micromanipulator (Oriel, Inc.; Märzhäuser GmbH) with the sensor tips 3 mm apart from each other. The microsensor tips were moved into the gradient capillary at its gas-filled side before the opening was covered with Vaseline (Fig. 1). The measured signals were connected to a computerized data acquisition system, which also controlled the micromanipulator (Unisense A/S). Horizontal profiles of oxygen and sulfide were measured with a step size of 100 or 200 μm. pH profiles were measured correspondingly by replacing the O_2 and the H_2S microsensors by the pH microsensor. The tip of the reference electrode was placed within the agar plug (Fig. 1).

Molar conversion ratio of sulfide oxidation within bacterial band. Molecular diffusion fluxes along the gradient capillary were determined according to Fick's first law for one-dimensional diffusion:

$$J(x) = D_0 \, \delta C(x)/\delta x \quad (3)$$

where D_0 is the free solution diffusion coefficient and $C(x)$ is the concentration of the solute at position x. Fluxes on both sides of the bacterial band were determined by linear regression of the measured concentration data within an interval of 500 μm next to the band. The change in flux across the band gave the uptake rate, R, of the bacterial band. The molar conversion ratio of sulfide oxidation (i.e., S_{tot}/O_2) was then given as:

$$S_{tot}/O_2 = R(S_{tot})/R(O_2) \quad (4)$$

The ratio of the diffusion coefficients of S_{tot} and oxygen was needed for this calculation. We used a value of $D_0(S_{tot})/D_0(O_2) = 0.757$ (4, 34).

Cell tracking, swimming velocity, and relative cell density. Swimming paths of motile cells were recorded on a digital video recorder (Sony, Inc.) with a charge-coupled device camera (EHD GmbH) attached to the microscope (Olympus BX50 WI). The focal plane was adjusted to the middle of the gradient capillary in order to exclude boundary effects of cells swimming near to the glass walls. The tracks and swimming velocities of individual cells were subsequently analyzed frame by frame (time steps, 0.04 s) by using the software program LabTrack (DiMedia, Kvistgård, Denmark). Tracks and swimming velocities reported in this study always represent their two-dimensional projections into the focal plane. An average swimming velocity was obtained by averaging the swimming velocities of all cell tracks ($n > 50$) within 1 s of a video recording.

Relative cell density distributions of motile cells were obtained by tracking over a time period of 2 s. The number of tracks within 50- or 200-μm intervals along the gradient capillary were taken as the relative cell density. Thus, only actively swimming cells were taken into account, if not otherwise stated. Relative cell densities of nonmotile cells could not be quantitatively analyzed with the existing system.

Photokinesis and photophobic response measurements. Capillaries with homogeneous oxic or sulfidic conditions were placed on the microscope stage and illuminated with 4.8 μmol of photons m^{-2} s^{-1} for 1 h before the photokinesis measurements at different irradiances were begun. Each irradiance was applied for 60 s before swimming velocities were measured by cell tracking over a period of 5 s.

For measurements of the photophobic response, a stepped neutral density filter was placed into the illumination path of the microscope so that the straight border between two different optically dense regions (optical density [OD] = 0 and OD = ~1) was projected into the microslide capillary.

RESULTS

General motility behavior. The polar flagellated cells of *M. gracile* always swam along their long axis. Straight swimming paths were interrupted by reversals in swimming direction. The cells stopped for ca. 0.04 s (corresponding to one frame of the video recording) before they resumed swimming in the opposite direction. The tracks before and after the reversal did not exactly coincide with each other. The two-dimensional projection of the angle between the tracks was on average 12.1° (standard deviation = 7.3°, $n = 24$). The motility patterns were apparently symmetrical with respect to both swimming directions.

Photokinesis was analyzed under oxic conditions, as well as under anoxic conditions, with 1 mM S_{tot} (Fig. 2A). In the first case average swimming velocities were not significantly influenced by irradiance and showed values of 33.4 ± 1.0 μm s^{-1}. The same was valid under anoxic conditions for >2 μmol photons m^{-2} s^{-1}, with swimming velocities of 34.0 ± 2.3 μm s^{-1}. Swimming velocities decreased to 19.5 μm s^{-1} at 0.05 μmol of photons m^{-2} s^{-1}. The dynamics of the swimming velocity in response to sudden changes in irradiance showed a biphasic behavior. The average velocity jumped within <1 s to a certain new value but kept changing within the next 60 to 120 s until a new steady-state value was achieved (see, for example, Fig. 2B).

M. gracile exhibited phobic responses toward different stimuli by reversing their swimming direction. Cells showed a photophobic step-down response when they crossed the border toward a less illuminated region, whereas cells crossing the border from the other direction did not show any response (Fig. 3A). Thus, cells were effectively trapped within the more intensive illuminated region. The photophobic response was not influenced by the oxygen or sulfide concentration. A phobic response was also observed toward certain lower and upper limits in oxygen or sulfide concentration. Figure 3B shows the response of swimming cells toward oxygen gradients in the dark. Cells swimming toward higher oxygen concentrations reversed their swimming direction at 6 to 10 μM O_2. Cells approaching from higher oxygen concentrations did not show the phobic response. Thus, cells accumulated within the microoxic region.

The reversals due to the photophobic response took place within a band of 20-μm thickness around the light-dark boundary (Fig. 3A). In the case of the phobic response toward oxygen, this band was ca. 100 μm thick (Fig. 3B). Otherwise the swimming tracks revealed no apparent difference between the photophobic response and the phobic responses toward oxygen or sulfide. All distribution patterns of *M. gracile* that are described below were caused by the phobic responses at the borders of the observed cell distribution.

Observations in gradient capillaries. The cells accumulated in a band of 500 μm thickness within opposing oxygen-sulfide gradients in the dark. The band was positioned between the oxic and the anoxic parts of the capillary (Fig. 4A). The boundary of the band toward the oxic part was found at ca. 10 μM.

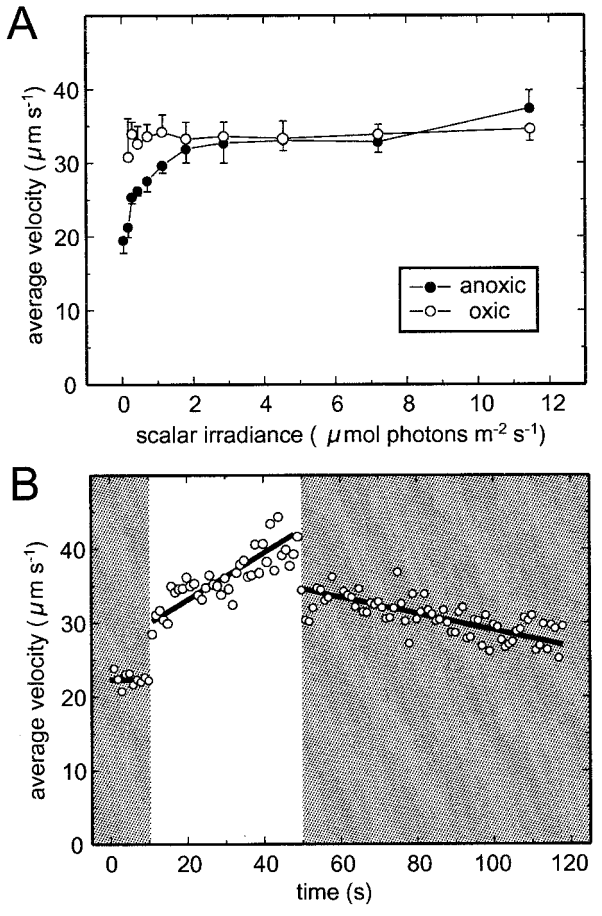

FIG. 2. (A) Photokinesis of *M. gracile* under oxic (>100 μM O_2) and anoxic (1 mM S_{tot}) conditions. Datum points represent the mean ± the standard deviation (n = 5) of the average swimming velocity. (B) Dynamics of photokinesis under anoxic (1 mM S_{tot}) conditions. The illumination intensity of 0.1 μmol of photons m^{-2} s^{-1} (shaded areas) was increased to 11.5 μmol of photons m^{-2} s^{-1} (bright area) for 30 s. The thick lines represent linear regressions.

More than 98% of the oxygen entering the band by diffusion was removed within the band (Fig. 4B). In contrast, S_{tot} was only partially removed within the band. The molar conversion ratio S_{tot}/O_2 for sulfide oxidation within the band was calculated to be 2.03:1. Preparations with different oxygen and sulfide gradients revealed that the position of the band was always at the oxic-anoxic interface independent of the sulfide concentration at this position (data not shown). The vertical band structure within the capillary could be revealed by moving the focal plane of the microscope through the inner space (0.8 mm in height) of the capillary. The cell density at the bottom was higher than at the top of the capillary, and the band position at the bottom was shifted 500 μm toward the oxic region relative to the band position at the top. There was no apparent difference in motility behavior between the cells in the top region and the ones in the bottom region. If the capillary was turned upside down, the vertical band structure readjusted within a few seconds. Again, the bottom part of the band showed the highest cell density and was shifted toward the oxic zone.

Only few nonmotile cells were observed in fresh gradient capillary preparations. If a preparation was kept for several hours, cells attached to the inner walls of the capillary. In the oxic part (>10 μM O_2) this was more pronounced at the bottom wall, where the bacteria formed small colonies consisting of 10 to 50 cells. No cells in their dividing stage could be observed by microscopic examination. In contrast, cells in the anoxic, sulfidic part attached preferably on the top wall but did not aggregate in colonies. Many of these cells were in their dividing stage.

If a bacterial band was illuminated with 18 μmol of photons m^{-2} s^{-1}, the cells retreated within 1 min toward the anoxic region. The dynamics of the migration are shown in Fig. 5A. Within the initial 5 s, the band broadened symmetrically toward both sides. After 10 s, the cells which were initially swimming into the oxic region, reversed their swimming direction. Thus, most cells had migrated toward the anoxic region after 50 s. In order to investigate the photophobic behavior in response to the dark-light transition, the illumination path was shaded every 1 s for ca. 0.25 s. The bacteria did not react to the shading immediately after the illumination was switched on. After 10 ± 2 s (n = 5), the photophobic response could be observed first, i.e., the cells reversed their swimming direction upon shading.

The retreat of the band was also examined in a different way by a stepwise increase of the irradiance (Fig. 5B). A weak irradiance of 0.2 μmol of photons m^{-2} s^{-1} did not significantly influence the bacterial band at the oxic-anoxic interface. At an irradiance of greater than ~10 μmol of photons m^{-2} s^{-1}, the band broadened and moved toward the anoxic region. The relative cell density still showed a maximum at its shoulder toward the oxic-anoxic interface, but there was no longer a sharp border toward the anoxic region. Eventually, all of the cells migrated toward the anoxic region when the irradiance was further increased.

The resulting steady-state situation for an illuminated (18 μmol of photons m^{-2} s^{-1}) gradient capillary with opposing oxygen and sulfide gradients is shown in Fig. 6A. Most of the swimming cells (>90%) were found in the region with <10 μM O_2. Apparently, the cells also avoided high sulfide concentrations, which resulted in a maximum of the cell distribution at an H_2S concentration of ~1.8 mM. If the oxygen was removed by flushing the surroundings of the gradient capillary with nitrogen, the cells migrated toward regions with less sulfide concentration. In the case of high sulfide concentrations (Fig. 6A), this migration finally resulted in an accumulation of all cells at the meniscus toward the gas-filled part of the capillary (data not shown). This migration stopped in the middle of the liquid culture medium if agar plugs with lower sulfide concentrations were prepared for the gradient capillary (Fig. 6B). A total of 67% of the cells accumulated in regions with <10 μM H_2S, where they formed a band positioned at the end of the sulfide gradient. Most of the sulfide diffusing through the gradient was removed within the bacterial band.

Dynamic changes of the oxygen and sulfide distribution could be observed in response to changing irradiance. Figure 7A shows the initial steady-state situation in the light (18 μmol of photons m^{-2} s^{-1}). The cells accumulated in the micro-oxic region (<10 μM O_2) close to the sulfidic agar plug. The oxygen penetration depth in the capillary was ca. 6 mm. The sulfidic and oxic zones overlapped within 2 mm. Upon darkening, the

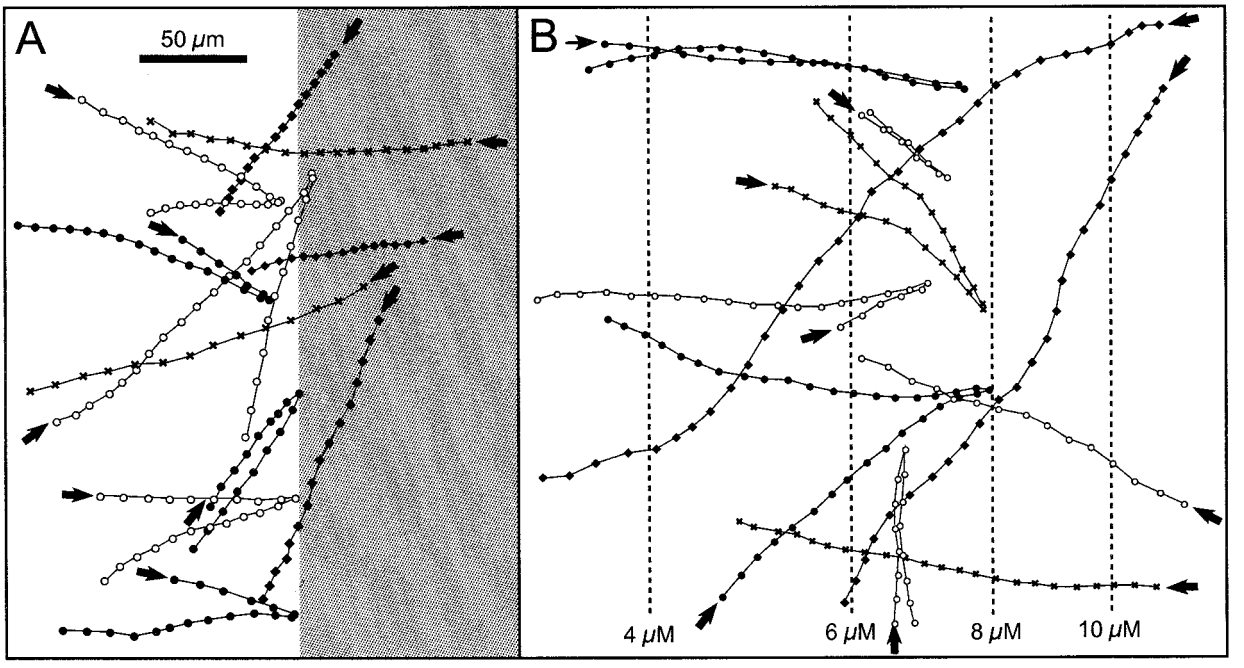

FIG. 3. Swimming tracks of single *M. gracile* cells. Points represent the positions of the cells with 0.04-s time steps. Various point symbols were used in order to distinguish the tracks of different bacteria. Arrows indicate the start of tracks. The scale bar in panel A is valid for both panels. (A) Photophobic step-down responses. Illumination intensities: 5 μmol of photons $m^{-2} s^{-1}$ (bright area) and ca. 0.5 μmol photons $m^{-2} s^{-1}$ (shaded area). (B) Phobic response toward exceeding oxygen concentrations. The dashed lines indicate oxygen isopleths.

cells migrated toward the oxic region and formed a band at the oxic-anoxic interface (Fig. 7B). After 1 h the position of the oxygen and sulfide gradients were shifted ca. 1.5 mm to the left, and the overlapping zone decreased to 1.5 mm. The steepness of the oxygen gradient increased from 41 to 50 μM mm^{-1}.

Observations under homogeneous conditions. In all previous experiments the cells were exposed to oxygen and sulfide gradients, wherein they could migrate to their "preferred" position. The sulfidic agar plug could sustain the sulfide gradient for ca. 24 h. Within this period the majority of cells did not lose their motility. In order to investigate the motility behavior under less favorable conditions (i.e., conditions which were avoided by the cells within oxygen or sulfide gradients), the cells were also exposed to homogeneous oxygen or sulfide concentrations. In the beginning of the following experiments all cells showed sulfur inclusions.

If the bacteria were exposed to 1 mM S_{tot} in the dark, they lost motility within 1 h and attached to the walls of the capillary. In contrast, the bacteria remained motile for >3 days if they were exposed to oxic conditions (>100 μM O_2) in the dark without any sulfide present, and many cells could be observed in their dividing state. After 5 days, only a few bacteria remained motile, while most had attached to the capillary walls. At this time the cells did not show any sulfur inclusions. When the cell density in such an oxic preparation in the dark was high enough, two bands of swimming bacteria separated by an anoxic region could be observed in the capillary (Fig. 8A). When the illumination (18 μmol of photons $m^{-2} s^{-1}$) was switched on, the bands approached each other and eventually merged. Within 30 min, the swimming cells concentrated to a dense spot ~300 μm in diameter (Fig. 8B and C). The oxygen concentration showed a minimum of 9.5 μM at the center of the spot. During the following 60 min, the spot broadened and finally measured 2 by 6 mm at steady state (Fig. 8D to G). The broadening was accompanied by an increase of the oxygen concentration, which reached ~40 μM at the center of the spot at steady state. Similar preparations with lower cell densities showed oxygen concentrations >100 μM at steady state in the light. Cells remained motile for >2.5 days. After 3 days, most of the cells were nonmotile and their sulfur inclusions had disappeared.

DISCUSSION

Photokinesis and phobic responses. Our photokinesis data point to a correlation of swimming velocity and the amount of energy supply in *M. gracile* (Fig. 2). Under oxic conditions and low irradiances the cells can compensate the diminished phototrophic energy supply by respiring their sulfur inclusions with molecular oxygen (31). The flagellar motor of bacteria is driven by the proton motive force across the cell membrane (Δp), which is built up as a result of photosynthetic and respiratory electron transport (1). ATP can also build up Δp via reverse activity of membrane-bound ATPase, and it was shown that externally supplied ATP increases the swimming velocity of *Rhodospirillum rubrum* (30). This might explain the biphasic velocity dynamics under anoxic conditions exhibited by *M. gracile* (Fig. 2), where the fast component of the dynamics was due to the direct coupling between the photosynthetic electron transport and Δp, whereas some intracellular energy storage, such as ATP, caused the slow component.

The motile behavior of *M. gracile* can generally be described

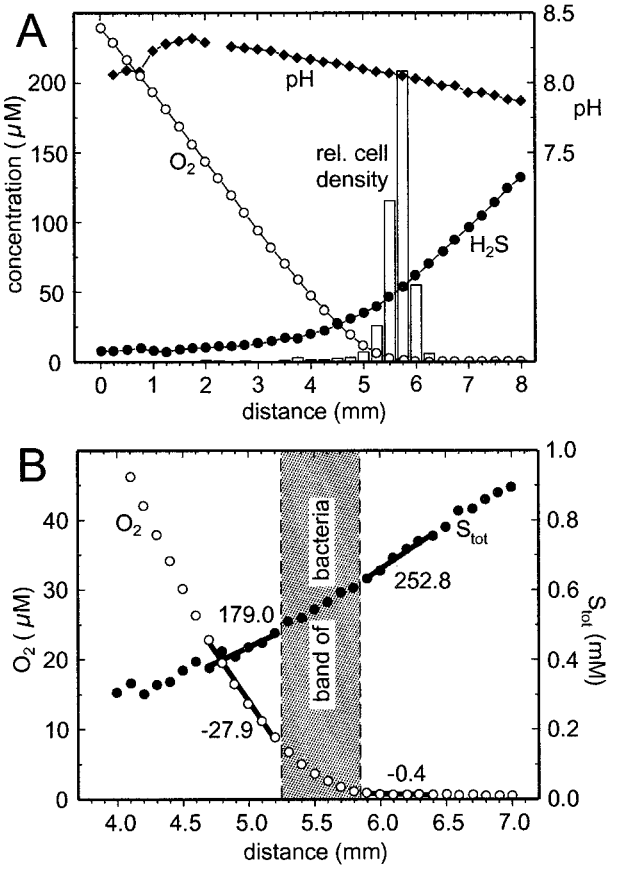

FIG. 4. (A) Relative cell distribution (bars, arbitrary linear units) of swimming *M. gracile* in the dark, together with oxygen (○), sulfide (●), and pH (◆) profiles. The *x* axis represents the distance along the long axis of the capillary. (B) Fine scale measurement of oxygen (○) and S_{tot} (●) profiles in the interval 4 to 7 mm of panel A. Thick lines represent linear regressions. The numbers next to the lines give their slope in micromolar units/millimeter.

as a random walk (2, 29). Intervals of straight swimming paths are interrupted by stops, followed by a reversal in swimming direction. Reversal probability is increased if the cell experiences a decrease in electron transport rate (1). In case of steep gradients, this behavior results in the observed phobic responses. A bacterium crossing the light-dark border produced by a stepped neutral density filter (Fig. 3A) experienced the full decrease in light intensity within 10 μm. Consequently, the reversal positions of the bacteria lie within a band of 20-μm width. Oxygen or sulfide gradients inside the gradient capillary always extended over several millimeters due to diffusional processes. This explains the less-sharp borders of the bacterial bands toward certain limits in oxygen or sulfide concentration (Fig. 3B).

The random walk pattern of *M. gracile* is different compared to the one exhibited by the enteric bacterium *Escherichia coli*, which interrupts its straight swimming paths by tumbling, resulting in a random direction change (2). *M. gracile* does not tumble but reverses its swimming direction. Thus, *M. gracile* is trapped within a region where it experiences local maxima of transfer rates in its electron transport chains. In contrast, the random direction changes of *E. coli* result in the possibility to move from one local maximum of chemoattractants to other local maxima. We speculate that this difference in motile behavior reflects the different habitats of the species. The habitats of *M. gracile* are characterized by light, oxygen, and sulfide gradients, where the simple reversal of swimming direction is sufficient to find maxima, which provide good growth conditions (e.g., the oxic-anoxic interface in darkness [Fig. 4]). In contrast, random direction changes are advantageous for *E. coli*, since enteric bacteria live in complex three-dimensional environments with many local chemoattractant maxima. Furthermore, Duffy and Ford (7) speculated that reversing swimming direction would lead to fewer bacterium-obstacle collisions in porous media, which might be advantageous for motility in benthic environments.

Engelmann (9) is generally regarded to be the first to have investigated the photoresponses of *Chromatium* spp. in the year 1883, when he described "*Bacterium photometricum*." The motility pattern of this bacterium was not symmetrical with respect to both swimming directions. Rather, straight swimming paths were interrupted by stops, followed by a short period with backward swimming. Thereafter, cells reoriented randomly, and resumed forward swimming. We observed a different motile behavior for *M. gracile*, a finding consistent with the observation made for *Allochromatium vinosum* by Mitchell et al. (29).

The dynamic behavior of *M. gracile* bacterial bands (Fig. 5A) indicates that the phobic response toward oxygen adapts under changing irradiance conditions. It took ca. 10 s before the band started to retreat toward the anoxic region, indicating that the phobic response to oxygen became active. The comparable adaptation times of ~10 s observed for the phobic responses toward light as well as toward oxygen point to a tight coupling. In accordance with the similar swimming patterns observed for phobic responses toward light and oxygen (Fig. 3), this underlines the theory that phototactic and chemotactic signaling are integrated by shared components in the electron transport chain of photosynthetic bacteria (1).

Motility behavior and metabolism in gradient chamber. In darkness *M. gracile* can grow chemotrophically if oxygen and reduced sulfur compounds are both present (21, 22). This explains the accumulation of the bacteria at oxygen levels between 0 and 10 μM in the zone where the oxygen and sulfide gradients overlap (Fig. 4). Kämpf and Pfennig (22) reported that the best chemotrophic growth conditions for *M. gracile* were 15 to 30 μM O_2, whereas higher concentrations caused cell lysis. Furthermore, oxygen concentrations of <10 μM still allow bacteriochlorophyll synthesis, which is suppressed at higher concentrations (22).

The two steps of sulfide oxidation are given by:

$$2H_2S + O_2 \rightarrow 2S^0 + 2H_2O \quad (5)$$

$$2S^0 + 2H_2O + 3O_2 \rightarrow 2SO_4^{2-} + 4H^+ \quad (6)$$

$$2H_2S + 4O_2 \rightarrow 2SO_4^{2-} + 4H^+ \quad (7)$$

The incomplete oxidation with S^0 as an endproduct requires 2 mol of sulfide for 1 mol of oxygen (equation 5), whereas for complete oxidation (equation 7) the S_{tot}/O_2 ratio is 1:2. The flux calculation for the bacterial band in the dark yielded a

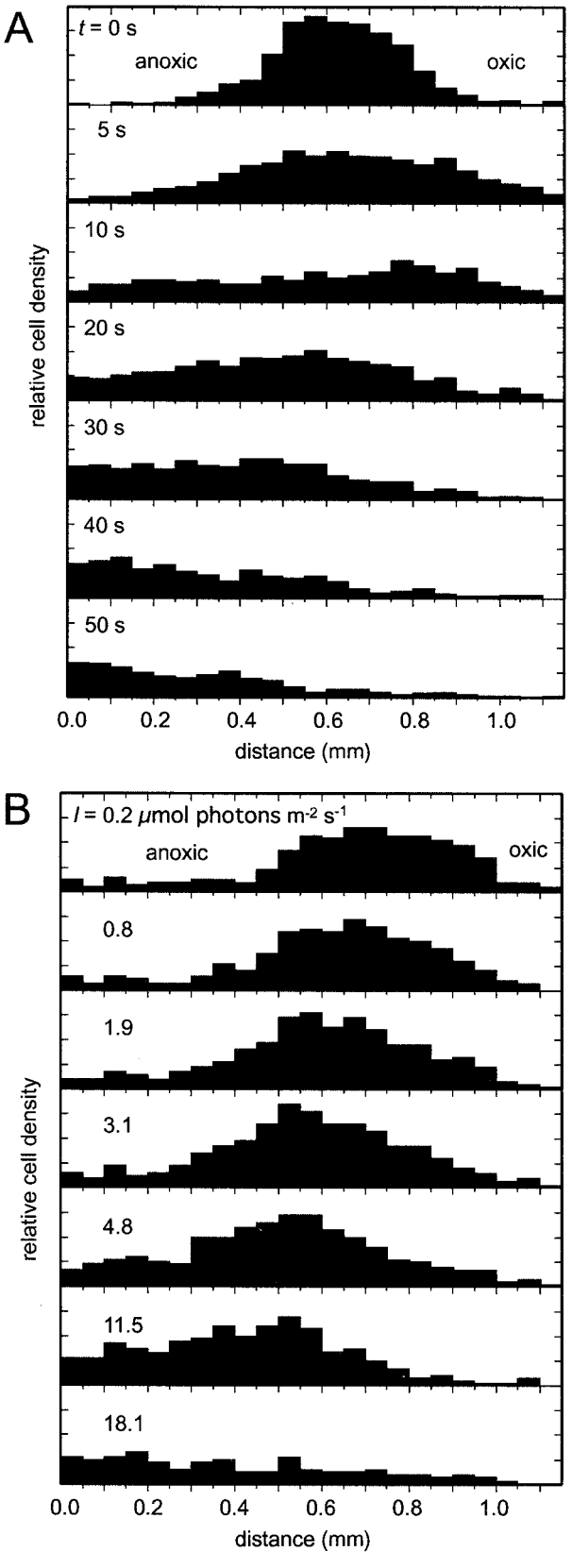

FIG. 5. Relative cell distribution (bars, arbitrary linear units) of swimming *M. gracile* at the oxic-anoxic interface. The *x* axis represents the distance along the long axis of the capillary. (A) Dynamics of the cell distribution in response to dark-light transition. The uppermost panel shows the steady-state distribution in the dark, where the band of bacteria was positioned between the oxic and the anoxic parts of the capillary. At time $t = 0$ s, the band was illuminated with 18 μmol of photons m^{-2} s^{-1}. The subsequent panels show the dynamics within the next 50 s. (B) Steady-state distributions at different irradiances (*I*).

S_{tot}/O_2 ratio of 2.03:1 (Fig. 4B). Thus, in the dark *M. gracile* oxidized sulfide, incompletely storing S^0 in its sulfur inclusions (32). Overmann and Pfennig reported molar conversion ratios of between 2.5:1 and 3.3:1 for other species of purple sulfur bacteria (31).

In the light *M. gracile* performs anoxygenic photosynthesis, which does not require the presence of oxygen. Thus, the bacteria spread into the anoxic part of the gradient capillary (Fig. 5B and 6A). The upper limit of the oxygen concentration was still ca. 10 μM, but the bacteria also preferred regions with low sulfide concentrations (Fig. 6B). Purple sulfur bacteria are well adapted to such low concentrations. Overmann reported K_m values for the oxygen and sulfide affinity of purple sulfur bacteria of 0.3 to 0.9 μM O_2 and 0.47 μM S_{tot}, respectively (31). Therefore, the bacteria can avoid possible harmful effects of high oxygen or high sulfide concentrations without limiting their substrate uptake rates.

All observed distribution patterns of *M. gracile* can be explained by its phobic responses toward light, oxygen, and sulfide. The photophobic response apparently overrules the other phobic responses, since shading caused a reversal in swimming direction of all bacteria independent of their position in the oxygen or sulfide gradient. Furthermore, the phobic response toward oxygen apparently overruled the one toward sulfide (Fig. 6).

The influence of *M. gracile*'s metabolism on its chemical microenvironment was seen under changing irradiance conditions. The oxygen respiration of the bacteria increased after a light-dark transition, and a steeper oxygen gradient indicated a higher oxygen flux (Fig. 7). Thus, the bacteria and the chemical gradients interact with each other. The distribution of the swimming cells is determined by the gradients, but the gradients are simultaneously influenced by the metabolism of the cells.

Motility behavior under adverse conditions. The interaction between the oxygen gradient and the cell's metabolism also caused the dynamic distribution pattern in the experiment shown in Fig. 8. At steady state in the dark, two bacterial bands removed all oxygen diffusing into the capillary and kept the space that was in between anoxic (Fig. 8A). As the respiration decreased in light, the oxygen concentration increased, forcing the motile bacteria to retreat and accumulate in the center (Fig. 8B to G). The bacteria were trapped within their self-generated oxygen minimum due to their phobic response toward oxygen. The highest bacterial density was observed when the oxygen distribution showed a minimum of ~10 μM O_2 (Fig. 8D), corresponding to the upper oxygen limit for the bacterial distributions in the gradient capillary. At this low oxygen level, the trapping mechanism works most effectively, but the number of accumulated bacteria was apparently not high enough to respire all oxygen diffusing toward the center. Consequently, the oxygen level increased until a steady state

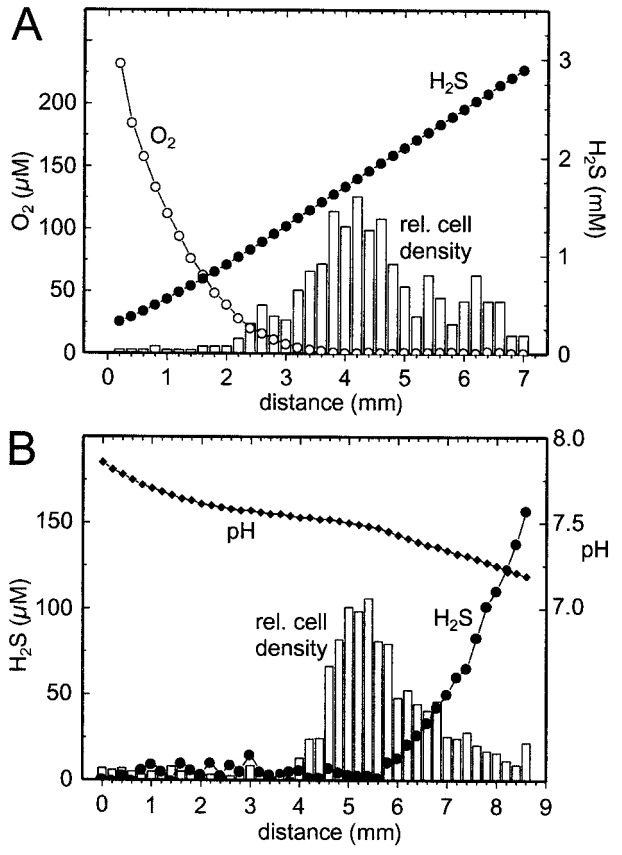

FIG. 6. Relative cell distribution (bars, arbitrary linear units) of swimming *M. gracile* in the light (18 μmol of photons m^{-2} s^{-1}), together with oxygen (○), sulfide (●), and pH (◆) profiles. The *x* axis represents the distance along the long axis of the capillary. (A) Oxic preparation with opposing oxygen and sulfide gradients (ca. 7.4 pH). (B) Anoxic preparation (oxygen replaced by nitrogen).

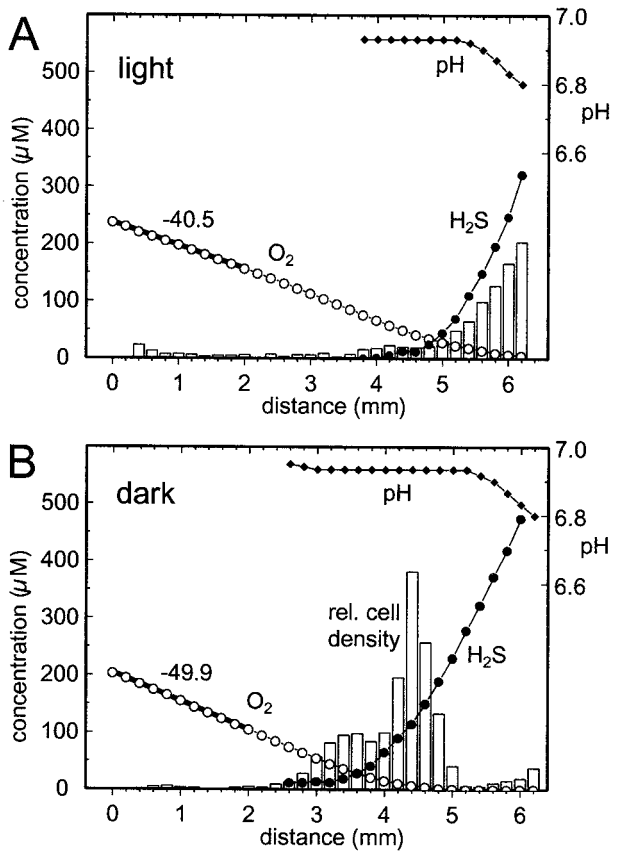

FIG. 7. Influence of changing illumination intensity on the relative cell distribution (bars, arbitrary linear units) of swimming *M. gracile* together with oxygen (○), sulfide (●), and pH (◆) profiles. The *x* axis represents the distance along the long axis of the capillary. The thick lines represent linear regressions. The numbers next to the lines give their slope in micromolar units/millimeter. (A) Steady state in light with 18 μmol of photons m^{-2} s^{-1}. (B) Situation after 1 h of darkness.

between respiration and oxygen influx was reached. The minimum of the steady-state oxygen profile (Fig. 8G) demonstrates clearly the ability of *M. gracile* to respire oxygen also in the light.

The latter observation might explain the formation of nonmotile colonies in the oxic part of the gradient capillary. Within colonies cells experience lower oxygen concentrations, reducing oxygen-related damage (22). The small colonies of 10 to 50 cells observed in our experiments are presumably not able to decrease the oxygen concentration significantly by their respiration. However, the experiment was conducted only over a period of several hours. Over longer periods the colonies may increase in size until oxygen is effectively removed by the respiring cells. This was, for example, observed by Seitz et al. (39) in a salt marsh where purple sulfur bacteria formed macroscopic aggregates on the sediment surface. Tidal currents exposed the aggregates periodically to oxic water, and microsensor measurements showed that the inner parts of the aggregates remained anoxic. The observed colony formation might also reflect the first stages of a biofilm formation.

Cells remained motile under oxic conditions for >2.5 days until their sulfur inclusions had disappeared. In darkness the bacteria presumably oxidize their sulfur inclusions to sulfate, whereas in the light anoxygenic photosynthesis with S^0 as an electron donor is performed (32). Although it was shown that *M. gracile* does not remain viable after long-term exposures to >50 μM O_2 (22), the demonstrated short-term resistance might be ecologically important. In their natural environment *M. gracile* can be exposed to high oxygen concentrations and the motile bacteria might be able to migrate, within the next several days, back to their favorite environment. Further, bacteria which get trapped in turbulent water above the oxic-anoxic interface can remain viable and may finally colonize other sulfidic habitats.

Under anoxic conditions in the dark it was shown that *Chromatium* spp. can generate ATP by oxidizing intracellularly stored glycogen to poly-β-hydroxybutyric acid. Elemental sulfur serves as an electron acceptor, and sulfide is released (41). The lower energy yield of this reaction compared to phototrophic or chemotrophic growth modes can explain our observation that *M. gracile* lost its motility under prolonged anoxia in the darkness.

The vertical band structure observed in the gradient capillary under dark conditions can be explained by the specific density of the cells. The specific density of *A. vinosum* cells with

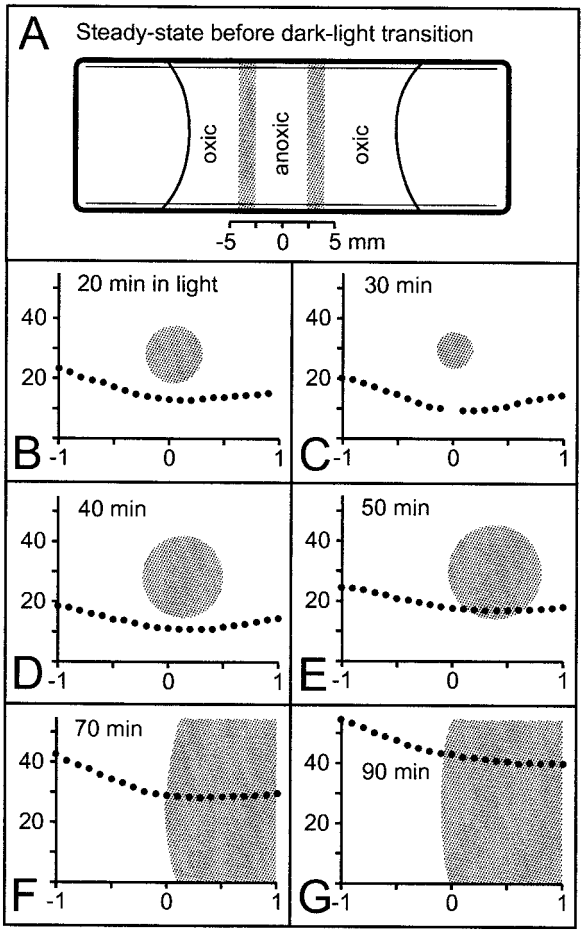

FIG. 8. Redistribution of swimming *M. gracile* (shaded areas) in response to a dark-light transition in the absence of sulfide. Note the different scales for panel A versus panels B to G. (A) Top view of flat microslide capillary with the steady-state distribution in the dark showing two bands of bacteria. (B to G) The bands merged to a single spot after the dark-light transition. Plots show oxygen profiles through the center of the spot within 90 min after illumination with 18 μmol of photons m^{-2} s^{-1} (*x* axis, millimeters; *y* axis, micromolar). Spot dimensions: given by the *x* axis in panels B to E; 2 by 3 mm^2 in panel F; and 2 by 6 mm^2 in panel G. The steady state in light was reached after 90 min.

sulfur inclusions was determined to be 16% higher than the density of water, resulting in a sinking rate of 0.12 μm s^{-1} (14). Negative buoyancy increases the probability that motile cells are found in the bottom part of the gradient capillary. Thus, the bottom part of the band exhibited a higher cell density accomplished with higher volumetric oxygen respiration rates than the upper part. The enhanced respiration rate at the bottom part leads to a shift of the 10 μM oxygen isopleth toward the oxic part of the capillary. Consequently, the bacterial band positioned itself along the isopleth resulting in the observed pattern.

Conclusions. Our investigation of *M. gracile* has identified a range of cellular motility responses that can explain migration patterns of purple sulfur bacteria in natural benthic habitats (19). The observed patterns result from phobic responses of the swimming bacteria. During night purple sulfur bacteria can move toward micro-oxic regions. If the oxic-anoxic interface is found below the surface, they presumably form an ~500-μm thin band at this position. In case of complete anoxia during night, sulfide is released into the overlaying water. In this case, no clearly defined oxic-anoxic interface can build up due to turbulent mixing in the water. Thus, the bacteria distribute as pink clouds in the overlaying water, where sulfide and oxygen are simultaneously present. During the daytime the oxic-anoxic interface moves into deeper layers due to oxygenic photosynthesis in the upper layers, and purple sulfur bacteria accumulate in a band below the oxic-anoxic interface. The upper limit of the band is given by 10 μM O_2, while the lower limit is determined by the attenuation of irradiance with depth (20). Additionally, *M. gracile* can withstand adverse conditions for several days, and the observed aggregation behavior provides a protection against high oxygen concentrations. Altogether, *M. gracile* is well adapted to dynamic changes in its habitat.

In line with earlier studies of colorless sulfur bacteria (11) and sulfate-reducing bacteria (10), the combination of gradient capillaries, microscopy, and microsensor measurements is a powerful approach for studying the motility behavior of single microorganisms, as well as the migration patterns of cell populations, under defined oxygen, sulfide, and light conditions. It allows the preparation of microenvironments, which mimic conditions found in sulfidic benthic habitats, and also allows the establishment of various stress scenarios. Microenvironmental conditions and metabolic rates can be quantified with microsensors at the same resolution at which simultaneous microscopy can reveal swimming patterns and band formation.

ACKNOWLEDGMENTS

This study was supported by grants from the European Commission (grants MAS3-CT98-5054 and EVK3-CT-1999-00010) and the Danish Natural Science Research Council (contract 9700549).

We thank Olivier Pringault and Henk Jonkers for providing media and for advice in handling the cultures. Remy Guyoneaud generously provided the culture of *M. gracile*. We thank Tom Fenchel, Andrea Wieland, and Nicholas Blackburn for advice regarding the gradient capillary setup, microsensor measurements, and video cell tracking, respectively. Finally, we thank Anni Glud for manufacturing excellent microsensors.

REFERENCES

1. **Armitage, J. P.** 1997. Behavioural responses of bacteria to light and oxygen. Arch. Microbiol. **168:**249–261.
2. **Berg, H. C., and D. A. Brown.** 1972. Chemotaxis in *Escherichia coli* analyzed by three-dimensional tracking. Nature **239:**500–504.
3. **Bernard, C., and T. Fenchel.** 1996. Behavioural responses in oxygen gradients of ciliates from microbial mats. Eur. J. Protistol. **32:**55–63.
4. **Broecker, W. S., and T. H. Peng.** 1974. Gas exchange rates between air and sea. Tellus **26:**21–35.
5. **de Wit, R., and H. van Gemerden.** 1987. Chemolithotrophic growth of the phototrophic sulfur bacterium *Thiocapsa roseopersicina*. FEMS Microbiol. Ecol. **45:**117–126.
6. **de Wit, R., and H. van Gemerden.** 1990. Growth of the phototrophic purple sulfur bacterium *Thiocapsa roseopersicina* under oxic/anoxic regimens in the light. FEMS Microbiol. Ecol. **73:**69–76.
7. **Duffy, K. J., and R. M. Ford.** 1997. Turn angle and run time distribution characterize swimming behavior for *Pseudomonas putida*. J. Bacteriol. **179:** 1428–1430.
8. **Eichler, B., and N. Pfennig.** 1988. A new purple sulfur bacterium from stratified freshwater lakes, *Amoebobacter pedioformis* sp. nov. Arch. Microbiol. **149:**395–400.
9. **Engelmann, T. W.** 1883. Bacterium photometricum: Ein Beitrag zur vergleichenden Physiologie des Licht und Farbensinnes. Arch. Gesamte. Physiol. Mensch. Tieres. Bonn **30:**95–124.
10. **Eschemann, A., M. Kühl, and H. Cypionka.** 1999. Aerotaxis in *Desulfovibrio*. Environ. Microbiol. **1:**489–494.

11. **Fenchel, T.** 1994. Motility and chemosensory behaviour of the sulphur bacterium *Thiovulum majus*. Microbiology **140:**3109–3116.
12. **Fonselius, S. H.** 1983. Determination of hydrogen sulphide, p. 73–80. *In* K. Grasshoff, M. Ehrhardt, and K. Kremling (ed.), Methods in sea water analysis. Verlag Chemie, Weinheim, Germany.
13. **Garcia-Pichel, F., and R. W. Castenholz.** 2001. Photomovements of microorganisms in benthic and soil microenvironments, p. 403–420. *In* D.-P. Häder and M. Lebert (ed.), Photomovement. Elsevier, Amsterdam, The Netherlands.
14. **Guerrero, R., J. Mas, and C. Pedrós-Alió.** 1984. Buoyant density changes due to intracellular content of sulfur in *Chromatium warmingii* and *Chromatium vinosum*. Arch. Microbiol. **137:**350–356.
15. **Häder, D.-P.** 1987. Photosensory behavior in prokaryotes. Microbiol. Rev. **51:**1–21.
16. **Hustede, E., M. Liebergesell, and H. G. Schlegel.** 1989. The photophobic response of various sulfur and nonsulfur purple bacteria. Photochem. Photobiol. **50:**809–815.
17. **Imhoff, J., J. Suling, and R. Petri.** 1998. Phylogenetic relationship among the Chromatiaceae, their taxonomic reclassification and description of the new genera *Allochromatium*, *Halochromatium*, *Isochromatium*, *Marichromatium*, *Thiococcus*, *Thiohalocapsa*, and *Thermochromatium*. Int. J. Syst. Bacteriol. **48:**1129–1143.
18. **Jeroschewski, P., C. Steuckart, and M. Kühl.** 1996. An amperometric microsensor for the determination of H_2S in aquatic environments. Anal. Chem. **68:**4351–4357.
19. **Jørgensen, B. B.** 1982. Ecology of the bacteria of the sulphur cycle with special reference to anoxic-oxic interface environments. Phil. Trans. R. Soc. Lond. Ser. B **298:**543–561.
20. **Jørgensen, B. B., and D. J. Des Marais.** 1986. Competition for sulfide among colorless and purple sulfur bacteria in cyanobacterial mats. FEMS Microbiol. Ecol. **38:**179–186.
21. **Kämpf, C., and N. Pfennig.** 1980. Capacity of Chromatiaceae for chemotrophic growth: specific respiration rates of *Thiocystis violacea* and *Chromatium vinosum*. Arch. Microbiol. **127:**125–135.
22. **Kämpf, C., and N. Pfennig.** 1986. Chemoautotrophic growth if *Thiocystis violacea*, *Chromatium gracile*, and *C. vinosum* in the dark at various oxygen concentrations. J. Basic Microbiol. **26:**517–531.
23. **Kohler, H.-P., B. Åhring, C. Albella, K. Ingvorsen, H. Keweloh, H. Laczkó, E. Stupperich, and F. Tomei.** 1984. Bacteriological studies on the sulfur cycle in the anaerobic part of the hypolimnion and in the surface sediments of Rotsee in Switzerland. FEMS Microbiol. Ecol. **21:**279–286.
24. **Kühl, M., and B. B. Jørgensen.** 1992. Microsensor measurements of sulfate reduction and sulfide oxidation in compact microbial communities of aerobic biofilms. Appl. Environ. Microbiol. **58:**1164–1174.
25. **Kühl, M., C. Lassen, and N. P. Revsbech.** 1997. A simple light meter for measurements of PAR (400 to 700 nm) with fiber-optic microprobes: applications for P vs. E_0 (PAR) measurements in a microbial mat. Aquat. Microb. Ecol. **13:**197–207.
26. **Kühl, M., C. Steuckart, G. Eickert, and P. Jeroschewski.** 1998. A H_2S microsensor for profiling biofilms and sediments: application in a acidic lake sediment. Aquat. Microb. Ecol. **15:**201–209.
27. **Lassen, C., H. Ploug, and B. B. Jørgensen.** 1992. A fibre-optic scalar irradiance microsensor: application for spectral light measurements in sediments. FEMS Microbiol. Ecol. **86:**247–254.
28. **Madigan, M. T.** 1988. Microbiology, physiology, and ecology of phototrophic bacteria, p. 39–111. *In* A. J. B. Zehnder (ed.), Biology of anaerobic microorganisms. John Wiley & Sons, New York, N.Y.
29. **Mitchell, J. G., M. Martinez-Alonso, J. Lalucat, I. Esteve, and S. Brown.** 1991. Velocity changes, long runs, and reversals in the *Chromatium minus* swimming response. J. Bacteriol. **173:**997–1003.
30. **Nultsch, W., and G. Throm.** 1968. Equivalence of light and ATP in photokinesis of *Rhodospirillum rubrum*. Nature **218:**697–699.
31. **Overmann, J., and N. Pfennig.** 1992. Continuous chemotrophic growth and respiration of Chromatiaceae species at low oxygen concentrations. Arch. Microbiol. **158:**59–67.
32. **Pfennig, N.** 1978. General physiology and ecology of photosynthetic bacteria, p. 3–18. *In* R. K. Clayton and W. R. Sistrom (ed.), The photosynthetic bacteria. Plenum Press, New York, N.Y.
33. **Pringault, O., R. de Wit, and M. Kuhl.** 1999. A microsensor study of the interaction between purple sulfur and green sulfur bacteria in experimental benthic gradients. Microb. Ecol. **37:**173–184.
34. **Pringault, O., E. Epping, R. Guyoneaud, A. Khalili, and M. Kühl.** 1999. Dynamics of anoxygenic photosynthesis in an experimental green sulphur bacterium biofilm. Environ. Microbiol. **1:**295–305.
35. **Revsbech, N. P.** 1989. An oxygen microelectrode with a guard cathode. Limnol. Oceanogr. **34:**474–478.
36. **Revsbech, N. P., and B. B. Jørgensen.** 1986. Microelectrodes: their use in microbial ecology. Adv. Microb. Ecol. **9:**293–352.
37. **Scherer, S.** 1990. Do photosynthetic and respiratory electron transport chains share redox proteins? Trends Biochem. Sci. **15:**458–462.
38. **Schlegel, H.** 1956. Vergleichende Untersuchungen über die Lichtempfindlichkeit einiger Purpurbakterien. Arch. Protistenkunde. **101:**69–98.
39. **Seitz, A. P., T. H. Nielsen, and J. Overmann.** 1993. Physiology of purple sulfur bacteria forming macroscopic aggregates in Great Sippewissett Salt Marsh, Massachusetts. FEMS Microbiol. Ecol. **12:**225–236.
40. **Sorokin, Y. I.** 1970. Interrelations between sulphur and carbon turnover in leromictic [sic] lakes. Arch. Hydrobiol. **66:**391–446.
41. **van Gemerden, H.** 1968. On the ATP generation by *Chromatium* in darkness. Arch. Mikrobiol. **64:**118–124.
42. **Wieland, A., and M. Kühl.** 2000. Short-term temperature effects on oxygen and sulfide cycling in a hypersaline cyanobacterial mat (Solar Lake, Egypt). Mar. Ecol. Prog. Ser. **196:**87–102.